Diffusion in Aqueous Gels. Mutual Diffusion Coefficients Measured by One-Dimensional Nuclear Magnetic Resonance Imaging

Bruce J. Balcom,† Alan E. Fischer, T. Adrian Carpenter, and Laurance D. Hall*

Contribution from the Herchel Smith Laboratory for Medicinal Chemistry, University of Cambridge School of Clinical Medicine, Cambridge CB2 2PZ, U.K.

Received September 9, 1992

Abstract: A simple, reliable method to measure mutual diffusion coefficients of paramagnetic species in aqueous gel media using one-dimensional nuclear magnetic resonance imaging is reported. The concentration variation with position of a paramagnetic marker yields a corresponding spatial variation in T_1 relaxation times within the gel. The inversion recovery imaging sequence employed nulls the image intensity from points in the gel with a specified T_1 value, which permits the position of any chosen marker concentration to be followed as a function of time. The experimental method minimizes the effect of T_2 relaxation in the gel. A plot of the null position as a function of the square root of time yields, after simple manipulation, the diffusion coefficient. The null point is well resolved with a characteristic signal variation in the vicinity of the null point. Diffusion coefficients of both organic (4-amino-TEMPO) and inorganic (copper sulfate) paramagnetic tracers in 10% polyacrylamide, 1% agarose, and silica gel media are reported.

Introduction

Diffusion coefficients are a fundamental measure of molecular mobility and as such may be used to probe the structure of a variety of gel networks.[1-8] We report here a new method, general in application, which provides a simple and reliable measure of mutual diffusion coefficients of paramagnetic solutes in aqueous gels using nuclear magnetic resonance imaging (NMRI). NMRI is well known[9-12] as a useful medical imaging modality but has only recently been used for analytical measurements on nonmedical systems. The sensitivity of NMRI to a large number of image contrast generating mechanisms has hindered its use in quantitative nonmedical applications where ideally one seeks a simple relationship between image intensity and a specific molecular property such as concentration. The null-point imaging sequence exploited herein yields a direct measure of paramagnetic solute concentration and position.

Theory/Simulation

The key feature which underlies this method is the simple relationship between spin-lattice relaxation rates and paramagnetic molecule concentration.[13] The induced relaxation of ^1H protons of water in the gel is a first-order process governed by eq 1,

$$1/T_1 = a + bC \tag{1}$$

where C is the concentration of the paramagnetic molecule, b is the molar relaxivity, and a is the inverse natural lifetime of water in this environment. A plot (Figure 1) of $1/T_1$ versus $[Cu^{2+}]$ in doped samples of 10% polyacrylamide gel gave a straight line ($r^2 = 0.99$) with a slope, b, of 0.814 s^{-1} mM^{-1} and an intercept, a, of 0.509 s^{-1}. The molar relaxivity varies widely between different paramagnetic species and is related to the number of unpaired electrons, the electron spin relaxation rate, and the rate of exchange between inner hydration sphere and bulk water.[14] The linear relationship of eq 1 is almost universally true[13] barring concentration-dependent phenomena such as precipitation and surface adsorption.

Given the linear relationship between paramagnetic concentration and spin-lattice relaxation rates, the concentration of a dilute paramagnetic species may be probed via its effect on the ^1H spin-lattice relaxation time (T_1) of the abundant, NMR-active, water protons in an aqueous gel. The inversion recovery[9] NMR imaging sequence (180°-t_d-90°-t_e/2-180°-t_e/2-acquire) yields a one-dimensional magnetization profile which is particularly sensitive to T_1 relaxation. The analytical expression for the signal intensity at a point is given by eq 2,

$$S = \rho \exp(-t_e/T_2)[1 - 2\exp(-t_d/T_1)] \tag{2}$$

where ρ is the proton density, t_e is the time until the spin echo is detected, and T_2 is the spin-spin relaxation time of the water. The variable t_d is an adjustable delay which will zero the third term in eq 2, and thereby the entire expression, when set equal to ($\ln 2T_1$). This relation is the basis of the simple null-point determination of T_1 in NMR spectroscopy.[15] Only the initial 180° inversion pulse and delay t_d distinguish this sequence from a standard spin echo imaging sequence.[16,17] Two-dimensional

† Current address: MRI Centre, Department of Physics, The University of New Brunswick, P.O. Box 4400, Fredericton, New Brunswick, Canada E3B 5A3.

(1) Dullen, F. A. *Porous Media Fluid Transport and Pore Structure*; Academic: London, 1979.
(2) Ogston, A. G.; Preston, B. N.; Wells, J. D. *Proc. R. Soc. London, A* **1973**, *333*, 297-316.
(3) Phillips, R. J.; Deen, W. M.; Brady, J. F. *J. Colloid Interface Sci.* **1990**, *139*, 363-373.
(4) Gibbs, S. J.; Johnson, C. S., Jr. *Macromolecules* **1991**, *24*, 6110-6113.
(5) Langdon, A. G.; Thomas, H. C. *J. Phys. Chem.* **1971**, *75*, 1821-1826.
(6) Bouaziz, J.; Woignier, J.; Bourret, D.; Sempere, R. *J. Non-Cryst. Solids* **1986**, *82*, 225-231.
(7) Davies, P. A. *J. Chromatog.* **1989**, *483*, 221-237.
(8) Yoon, H.; Kim, H.; Yu, H. *Macromolecules* **1989**, *22*, 848-852.
(9) Callaghan, P. T. *Principles of Nuclear Magnetic Resonance Microscopy*; Oxford Science: Oxford, England, 1991.
(10) Listerud, J. M.; Sinton, S. W.; Drobny, G. P. *Anal. Chem.* **1989**, *61*, 23A-41A.
(11) Kuhn, W. *Angew. Chem., Int. Ed. Engl.* **1990**, *29*, 1-19.
(12) Attard, J. J.; Carpenter, T. A.; de Crespigny, A.; Duce, S. L.; Hall, L. D.; Hawkes, R. C.; Hodgson, R. J.; Herrod, N. J. *Philos. Trans. R. Soc. London, A* **1990**, *333*, 477-485.
(13) Abragam, A. *The Principles of Nuclear Magnetism*; Oxford Science: Oxford, England, 1989; p 328.
(14) Lauffer, R. D. *Chem. Rev.* **1987**, *87*, 901-927.
(15) Sanders, J. M.; Hunter, B. K. *Modern NMR Spectroscopy*; Oxford University Press: Oxford, England, 1989; p 182.
(16) Reference 9, p 292.
(17) Hall, L. D.; Rajanayagam, V. *J. Magn. Reson.* **1987**, *74*, 139-146.

0002-7863/93/1515-3300$04.00/0

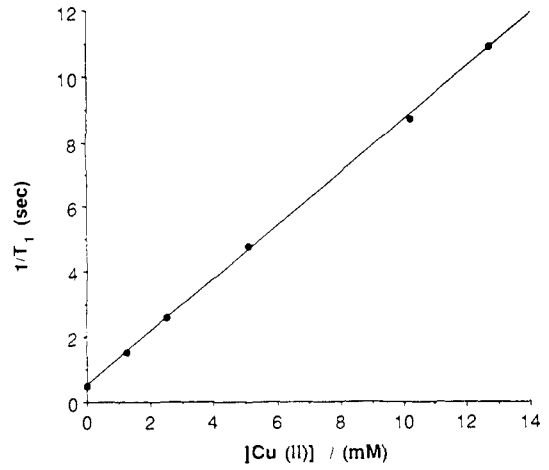

Figure 1. Plot of inverse T_1 versus copper sulfate concentration. The relation is linear, according to eq 1, with a slope, b, of 0.810 mM^{-1} s^{-1} and an intercept, a, of 0.509 s^{-1}.

inversion recovery imaging sequences have recently been used to give enhanced T_1 contrast in conventional NMRI.[17,18]

The sequence outlined above will localize a chosen paramagnetic concentration in a sample without regard to its spatial variation. In this work the spatial variation of concentration is governed by the one-dimensional diffusion equation with boundary conditions (free diffusion into a semi-infinite slab from a constant concentration reservoir) chosen to yield a simple result,[19] eq 3,

$$C/C_0 = \mathrm{erfc}[x/2(Dt)^{1/2}] \qquad (3)$$

for which C/C_0 is the normalized concentration, D the diffusion coefficient, x the spatial position, and t the elapsed time of the experiment. The boundary conditions above require that the reservoir solution in the diffusion cell be well mixed and of fixed concentration. In practise, random mixing due to small temperature fluctuations and to vibration induced by the gradient coils ensure the reservoir solution is well mixed. Limiting the duration of the experiment ensures C_0 remains essentially constant (5% decrease in 90 min for a typical measurement).[20] Equation 3 also requires, and we achieve, a sharp initial boundary between gel and reservoir. Fortunately the gel network, by its nature, limits convective mixing, so diffusion alone occurs in the gel.

Figure 2 shows the solution to eq 3 at four experimental times, 200, 1000, 2500, and 5000 s, for a diffusion coefficient of 3.0×10^{-6} cm^2 s^{-1}. Our approach is to follow a concentration contour $C = C'$, determined by t_d, which is a small fraction of the reservoir concentration C_0. A plot of the position of C' versus the square root of time will yield the diffusion coefficient D directly after simple regression analysis. As shown in Figure 2, a small C'/C_0 ratio is desirable in order to achieve the maximum displacement in the minimum time. Ideally one would track an infintely small C'; however, resolution of the null point is difficult, vide infra, and the estimate prone to error in this limit.

The experiment may be simulated by combining eqs 1, 2, and 3 and exploring the effect of altering the experimental variables. Two features should be noted. Although points with T_1 values greater than $t_d/\ln 2$ should have negative signal intensities, because our experimental data is magnitude data, the simulated signal intensities are plotted as absolute values. In addition, the values of the first two terms in eq 2 are set to unity. The first term, ρ, is the normalized proton density, which is spatially invariant and therefore may be set to 1. Setting the second term equal to 1 assumes that T_2 is very long in the gel. This is not always true,

(18) Young, I. R. In *Practical NMR Imaging*; Foster, M. A., Hutchinson, J. M., Eds.; IRL Press: Oxford, England, 1987; pp 145–171.
(19) Crank, J. *The Mathematics of Diffusion*; Oxford Science: Oxford, England, 1989; p 21.
(20) Reference 19, p 21.

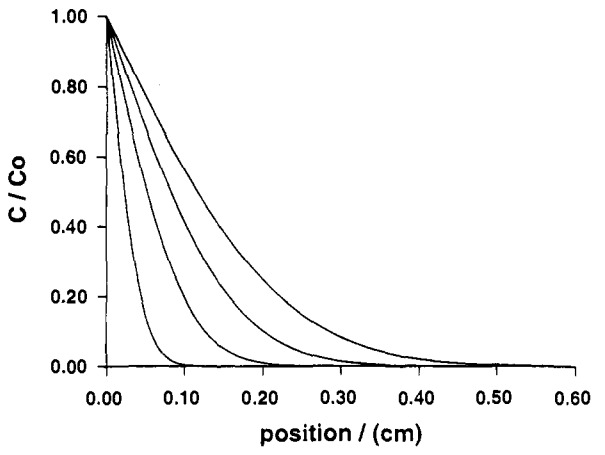

Figure 2. Solution to eq 3 at times 200, 1000, 2500, and 5000 s. The plot of concentration versus position was generated with $D = 3.0 \times 10^{-6}$ cm^2 s^{-1}. Note that the position of any chosen C/C_0 is displayed a greater distance in a given time the smaller the value of C/C_0. Similarly the slope dC/dx decreases with time for all C/C_0.

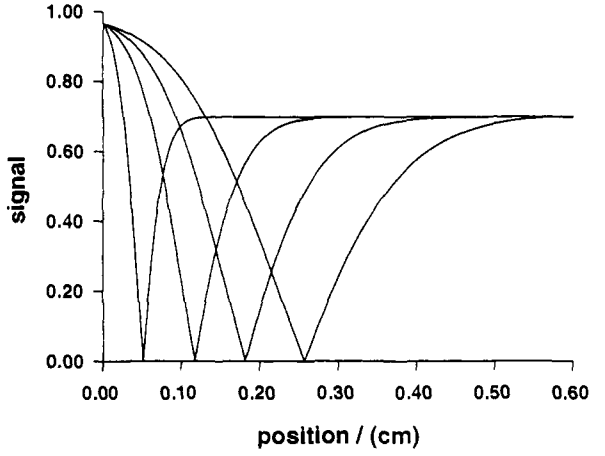

Figure 3. Simulation of the inversion recovery null-point diffusion experiment. The simulation conditions are C_0 = 15 mM and C' = 2.0 mM with a diffusion coefficient of 3.0×10^{-6} cm^2 s^{-1}. The experimental times are those of Figure 2. Note the symmetry of the curve about the null point and the breadth of the curve, which increases with time. The delay time τ_d is calculated according to eq 1 with $\tau_d = \ln 2T_1$ for C' = 2.0 mM.

and since it is an important issue with respect to the general applicability of the technique, it will be considered further below.

Figure 3 is a series of four simulated NMR profiles where the signal is plotted as a function of position at times corresponding to those of Figure 2. The C_0 concentration was 15.0 mM, the tracked C' was 2.0 mM, and the diffusion coefficient was 3.0×10^{-6} cm^2 s^{-1}. Several features of the model experiment are immediately apparent. The signal intensities at $x = 0$ and $x \rightarrow \infty$ are not 1. This is expected, since the recoveries of the magnetization vectors at these two points are governed by their respective inverse T_1 values, which are $a + bC_0$ and a. These values are neither much longer than t_d nor much shorter than t_d, where $t_d = \ln 2/(a + bC')$, which would be the criteria for either complete recovery or no recovery during t_d. Most striking, however, is the form of the signal near the null point. At all times the signal is symmetric in the region of this point; the null point is well defined but the neighboring curve broadens with time. The excellent definition of the null point in these simulations suggests that, given adequate signal-to-noise, the null point should be easily tracked experimentally.

Simulations, not shown, indicate that the best definition of the null point is achieved when the signals at points $x = 0$ and $x \rightarrow \infty$ are roughtly equivalent. This restriction is quite loose in

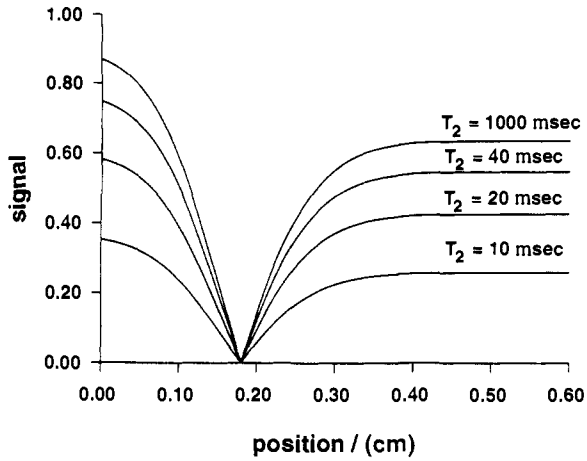

Figure 4. Simulation result showing the effect of T_2 on resolution of the null point in an inversion recovery null point tracking experiment. Simulation conditions are those of Figure 3 at time 2500 s. The second term of eq 2 is added to the simulation for model T_2 values of 1000, 40, 20, and 10 ms with an echo time of 10 ms. Localization of the null point will be more difficult as T_2 decreases.

practise, since experimentally we observe adequate resolution when these two levels are within no more than 50% of one another. For a given paramagnetic with molar relaxivity b and a medium with inverse natural lifetime a, the signals at points $x = 0$ and $x \rightarrow \infty$ will be roughly equivalent when $bC' \geq 3a$. Since b and a are known from a calibration curve, the tracked concentration C' is readily calculated, and since C'/C_0 is $\sim 1/8$, this leads directly to the required reservoir concentration. The variable delay t_d is calculated directly by the formula $t_d = \ln 2/(a + bC')$. These guidelines account for variations in both probe and gel properties.

As previously stated the null point will be most easily detected experimentally when the signal-to-noise in the neighboring pixels is high. An important restriction on the signal-to-noise will be the T_2 of the sample, which influences the experiment via the second term in eq 2. Figure 4 is a plot of signal intensity versus position, in a model experiment, for various T_2 values of the gel matrix. Clearly, decreasing T_2 will decrease the slope of the curve through the null point, thereby hindering identification of this point when a moderate amount of random noise is present. It should be noted that this T_2 must be measured by a Hahn spin echo not a CPMG[21] sequence, since a Hahn spin echo is used in the imaging experiments. One should also note that, in general, the T_2 value in the gel will not be spatially invariant due to the dependence of T_2 upon paramagnetic concentration;[13] this will not greatly alter the experiment because a very short echo time t_e is typically chosen. The simple one-dimensional profile experiment is more favorable in terms of signal-to-noise than a two- or three-dimensional image because the profile method sums the signal intensity from all points a distance x from the interface and furthermore the echo time is minimized in the absence of a slice select gradient.

Results and Discussion

Figure 5 shows the results of a representative diffusion experiment at three discrete times. In this case Cu^{2+} is diffusing from right to left into a cylinder of 10% polyacrylamide gel. Figure 6 shows a plot of the position of C' versus the square root of time for a similar Cu^{2+} diffusion experiment where the observations of four concentrations C' (1.0, 2.0, 3.0, and 6.0 mM) have been interleaved. The linearity of the plots in Figure 6 confirms that copper ions spread through the gel via a diffusion mechanism. The intercept of the best fit line in each case yields a measure of the interface between the gel and reservoir solution. The slope, as mentioned previously, yields the diffusion coefficient.

(21) Meiboom, S.; Gill, D. *Rev. Sci. Instrum.* **1958**, *29*, 688–691.

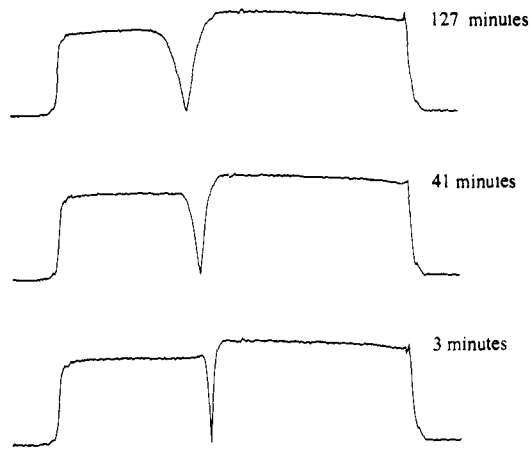

Figure 5. Experimental one-dimensional magnetization profiles, as a function of time, showing aqueous diffusion of Cu^{2+} into 10% polyacrylamide. Null point is 2.0 mM; field-of-view is 5.21 cm with 256 points in each profile. The gel sample is on the left, $CuSO_4$ reservoir on the right. Interface is 2.36 cm from the left edge of each profile.

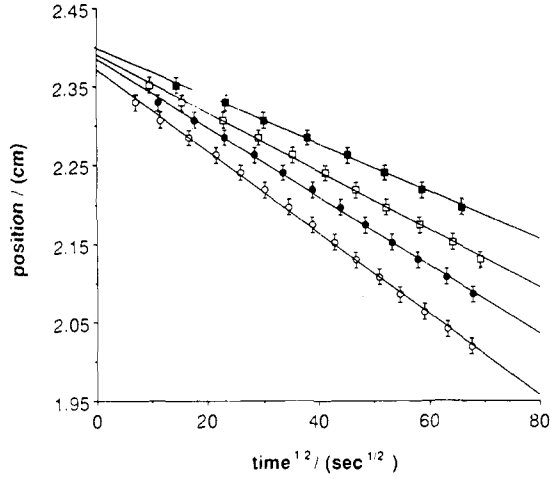

Figure 6. Position of null points C' corresponding to 1.0 (○), 2.0 (●), 3.0 (□), and 6.0 (■) mM Cu^{2+} plotted versus $t^{1/2}$ for a diffusion experiment in 10% polyacrylamide. Uncertainty in the position is $\pm 1/2$ pixel (0.1 mm). The intercept is the estimated interface between gel and the $CuSO_4$ reservoir (C_0 = 15.0 mM). The average D from this experiment, derived from the slope, is 3.5×10^{-6} cm^2 s^{-1}.

Clearly these four slopes are significantly different from one another; however, the differences is offset by the normalized concentration C'/C_0 in eq 3, which is different in each of the four cases. The net result (polyacrylamide experiment 7, Table I) is four diffusion coefficients which are in close agreement.

Examination of the profiles in Figure 5 reveals several significant features of the experiment. (1) Unlike a conventional spectroscopic inversion recovery experiment, the signal intensity is always positive. As discussed in the previous section, a magnitude Fourier transform of the NMR data yields the absolute value of the signal given by eq 2; magnitude data is preferred because it avoids the necessity of phasing the data. The region of the sample which should have negative signal intensity is the bulk gel on the left-hand side of the profiles in Figure 5 which has a long T_1 value. (2) The null point is well resolved and closely approximates zero, which is an experimental verification of the simulation results presented earlier. However, the signal will approximate zero only when the distribution of T_1 values within the volume defined by a pixel is very narrow. At very early times in an experiment, when the concentration gradient around C' is very large, the signal intensity will not be zero; nevertheless it will be a minimum, and this is a sufficient condition to mark the position of C'. (3) The curve is symmetrical in the vicinty of the

Table I. Cu^{2+} Diffusion Coefficients

gel	experiment[a]	$D/(10^{-6}$ cm^2 s$^{-1})$
10% polyacrylamide	1	3.0
	2	3.5
	3	3.5
	4	3.1
	5	3.4
	6	3.0
	7[b]	3.5
		3.4
		3.4
		3.6
1% agarose	1	4.8
	2	4.9
	3	4.8
	4	4.8
	5	4.8
	6[c]	4.6
		4.7
		4.6
silica	1[d,e]	3.2
		3.5
		3.8
		3.1

[a] Except where noted, $C' = 2.0$ mM, $C_0 = 15.0$ mM, and $T = 21.5 \pm 0.5$ °C. [b] Multiple concentrations C' tracked (1.0, 2.0, 3.0, 6.0 mM). [c] Multiple concentrations C' tracked (1.4, 2.2, 3.6 mM). [d] $C_0 = 85$ mM, $T = 27 \pm 0.5$ °C. [e] Multiple concentrations C' tracked (6.6, 8.3, 13, 21 mM).

null point. The spatial derivative of eq 2 (first two terms set to unity) at the null point, $S = 0$, is given by eq 4,

$$dS/dx = bt_d\, dC/dx \tag{4}$$

which assumes that the proton density, ρ, is constant and a short t_e masks any spatial dependence of T_2. The differential of the absolute signal intensity is therefore directly proportional to the differential paramagnetic concentration in the region of the null point. Since the variation of concentration with position is approximately linear over small distances (Figure 2), the curve is symmetrical about the null point. (4) The breadth of the curve in the vicinity of the null point increases with time. The value of the derivative dC/dx (Figure 2), evaluated at C' where $S = 0$, decreases as the concentration C' moves further from the origin, and therefore dS/dx decreases.

Our consideration of the experiment to this point has focused on smooth analytical functions of space and time and has neglected the discrete nature of the data collected. A finite number of data points, typically 256 or 512 points, may not adequately reconstruct a function which changes value rapidly. The only region of the sample where this causes concern is the null point. Examination of the signal intensity from points on either side of an experimental null point shows the signal is often highly asymmetrical, which is at variance with both the simulated data and eq 4. The asymmetry is due to the finite size of the pixels (0.2 mm) which are used to reconstruct the true experimental data. Unless the true null point at high resolution coincides with the center of a pixel, the signals from pixels either side of the null point will have different values because the inherently symmetrical data is asymmetrically sampled by the pixels used in the reconstruction. Since the true null point will traverse a given pixel in a finite amount of time, by sampling discrete profiles at time intervals on the order of tens of seconds, one will assemble a series of profiles where the experimental minimum is localized in the same pixel; but progressing through the time series, the asymmetry is skewed first one way then the other with the median profile invariably showing the best symmetry about the null point. This is expected if the null point moves with constant velocity through that pixel, which is a reasonable approximation over a distance the size of a pixel. However the velocity should decrease with time, which suggests the null point will be resident in a given pixel for a longer period of time the further the null point moves from the origin; this was observed experimentally. The practical manifestations of this pixelation effect are threefold. The uncertainty in the null point is somewhat less than the width of a pixel, as estimated in Figure 6. Because we have a criterion for 'good' null point estimates, namely symmetry, the semi-automated method of data analysis yields excellent results. Furthermore, since the median profile of such a series is the best estimate, the automated data analysis method (using all 128 profiles) gives results essentially the same as the semi-automated method.

Several other laboratories have recently used the dependence on paramagnetic tracer concentration of water relaxation times to measure diffusion coefficients in porous media.[22-24] The weakness of all three methods is the effect of T_2 on the measurement. Pearl et al.[23] are restricted to media which have very short T_2 values such that only T_1 varies spatially while Guillot et al.[22] are restricted to a narrow concentration range where a given combination of the repetition time and echo time yield a signal directly proportional to concentration. Asakura et al.[24] have attempted to take account of the explicit concentration dependence of T_2; however, one should note that, in a microscopically heterogeneous medium like a gel, the measured T_2 will generally be dependent on the sequence used.[25,26] Certainly a CPMG sequence[21] is unlikely to give the same answer as a Hahn spin echo with a pulse spacing analogous to that of an imaging experiment. Underlying the special conditions which the first two studies used to minimize the T_2 effect is the subtle dependence of the imaging experiment on a wide variety of contrast-generating mechanisms which involve T_2. Clearly the best experiment is one which is free of special restrictions, as far as possible, and is applicable to the broadest range of substrates. The inversion recovery sequence, used in the present study, by employing a null measurement neatly avoids the troublesome behavior of T_2. In addition, the form of the data leads to a simple plot of x versus $t^{1/2}$, from which linear regression yields a diffusion coefficient directly. The alternative approach, whereby one assembles a concentration versus position curve at a given time, requires nonlinear regression to yield D. We note in passing that the inversion recovery imaging sequence may be used to reconstruct a concentration curve at a specified time in the diffusion experiment by stepping the delay t_d through a series of values which correspond to known concentrations. By successive application of this sequence, a plot of the position of the chosen concentrations may be assembled, provided the overall curve does not change during data acquisition. Figure 7 shows the result of such an experiment 171 min after initiation of diffusion; overlaid are concentration points calculated from eq 3 using an experimental diffusion coefficient determined in the early part of the experiment by the null point tracking method. Although the agreement is encouraging, the experiment in general is less satisfactory because it requires a good estimate of the gel/reservoir interface, is restricted to long experimental times, and requires nonlinear regression to determine D.

The motivation for this study, and the resulting experiments, is our involvement in reaction and diffusion measurements of paramagnetic contrast agents in a variety of ideal and nonideal porous media.[27,28] For this reason we required fundamental data on the diffusion coefficients of representative contrast agents in

(22) Guillot, G.; Kassab, G.; Hulin, J. P.; Rigord, P. *J. Phys. D* **1991**, *24*, 763–773.
(23) Pearl, Z.; Magaritz, M.; Bendel, P. *J. Magn. Reson.* **1991**, *95*, 597–602.
(24) Asakura, T.; Demura, M.; Ogawa, H.; Matsushita, K.; Imanari, M. *Macromolecules* **1991**, *24*, 620–622.
(25) Zhong, J.; Gore, J. C.; Armitage, I. M. *Magn. Reson. Med.* **1989**, *11*, 295–308.
(26) Kurland, R. J.; Ngo, F. Q. *Magn. Reson. Med.* **1986**, *3*, 425–431.
(27) Balcom, B. J.; Carpenter, T. A.; Hall, L. D. *J. Chem. Soc., Chem. Commun.* **1992**, 312–313.
(28) Balcom, B. J.; Carpenter, T. A.; Hall, L. D. *Can. J. Chem.*, in press.

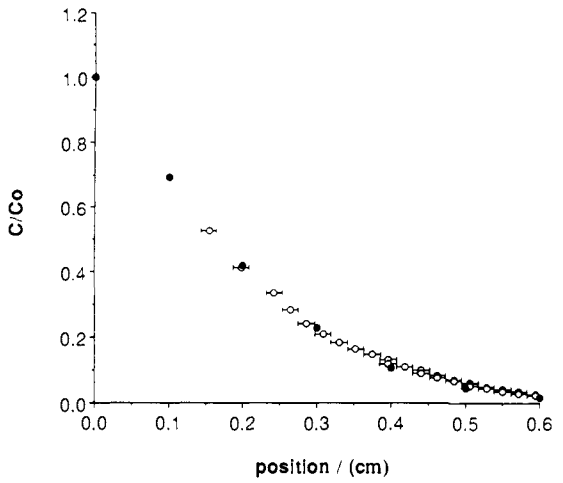

Figure 7. Normalized concentrations C/C_0 (○) plotted versus position 171 min after initiation of 15.0 mM Cu^{2+} diffusion into 10% polyacrylamide. Discrete concentrations C, and therefore C/C_0, were localized by null-point determination at many different times τ_d. Overlayed are normalized concentration points C/C_0 (●) calculated according to eq 3 for $D = 3.0 \times 10^{-6}$ cm^2 s^{-1}. Uncertainty in each position estimate is $\pm 1/2$ pixel (0.1 mm).

Table II. 4-Amino-TEMPO Diffusion Coefficients

gel	experiment[a]	$D/(10^{-6}$ cm^2 s$^{-1})$
10% polyacrylamide[b]	1[c]	2.5
		2.4
		2.3
		2.1
	2[c]	2.6
		2.7
		2.7
		2.6
	3[c]	2.8
		2.9
		3.0
		3.0
	4[c]	2.9
		3.1
		2.9
		3.0
1% agarose[d]	1	3.8
	2	3.6
	3	4.0
	4	4.3
	5	4.3

[a] $T = 21.5 \pm 0.5$ °C. [b] $C_0 = 57$ mM. [c] Multiple concentrations C' tracked (1.1, 3.3, 6.0, 10 mM). [d] $C_0 = 51$ mM, $C' = 10$ mM.

a number of media. These studies were also intended to test the applicability of the technique to a number of experimental environments. The experimental diffusion data are summarized in Tables I and II. The probes employed were copper sulfate (Table I) and 4-amino-TEMPO (Table II). The gel matrices examined are 10% polyacrylamide, 1% agarose, and silica gel. Polyacrylamide and agarose are commoly used in biotechnology applications,[29-31] gel electrophoresis,[32,33] and chromatography.[34,35] They have very different pore diameters, but water in each gel has a long T_1 value (seconds) and a short T_2 value (low hundreds of ms). [Spin–lattices relaxation times (T_1) measured by an inversion recovery sequence. Spin–spin relaxation times (T_2) measured by a Hahn spin echo sequence.] Silica gel is also a common chromatography medium and has short aqueous T_1 (hundreds of ms) and very short T_2 (tens of ms).

The optimum concentrations C' for these experiments were calculated according to the rules developed in the simulations, viz. $bC' \geq 3a$ with $C'/C_0 \sim 1/8$. Since copper sulfate has a molar relaxivity, b, approximately 4 times greater than 4-amino-TEMPO (0.810 s^{-1} mM^{-1} versus 0.210 s^{-1} mM^{-1} for 10% polyacrylamide, comparable results in 1% agarose), C' and also C_0 must increase for an experiment with 4-amino-TEMPO. Silica gel has a natural lifetime, T_1, in the absence of relaxation agent which is much shorter than that of 10% polyacrylamide (200 ms versus 2 s) hence the value of a in the calibration curve is much larger. Therefore, for the same nominal resolution of the null point, with a molar relaxivity which is media invariant, the observed concentration C', and therefore C_0, must be proportionally higher.

We have examined the reproducibility of our experimental results in two ways; first a series of measurements over several days using different gel preparations, and second a series of measurements on the same day with one gel preparation. The first series of measurements are polyacrylamide experiments 1–6 in Table I; the second series of experiments, which show much less variation, are agarose experiments 1–5 also in Table I. The uncertainty in an individual experiment is approximately 5%, as calculated from the uncertainty in the x versus $t^{1/2}$ plots and the uncertainty in C' from the calibration curve. The polyacrylamide gel results prove that the uncertainty in individual experiments is not, in general, the major source of experimental error; rather, day to day variability in performing the experiment and formulating the samples dominates.

The pooled results of Table I give diffusion coefficients (and 95% confidence intervals) for copper ion diffusion into the three experimental media. In a 10% polyacrylamide matrix the diffusion coefficient is $(3.3 \pm 0.2) \times 10^{-6}$ cm^2 s^{-1}, whereas in 1% agarose the diffusion coefficient is $(4.8 \pm 0.1) \times 10^{-6}$ cm^2 s^{-1}. In a silica gel medium, with fewer measurements, the diffusion coefficient is $(3.5 \pm 0.5) \times 10^{-6}$ cm^2 s^{-1}. Qualitatively the diffusion coefficient of Cu^{2+} in silica gel is similar to the result in 10% polyacrylamide. This is not wholly surprising because the average pore size in the two media is very similar. For both 10% polyacrylamide and silica gel, the average pore size is on the order of tens of cubic nanometers.[36,37] Localization of the null point in the silica gel experiment was difficult due to the poor signal-to-noise of the experimental profiles. The T_2 of the silica gel matrix, measured with a Hahn spin echo, was 20 ms and, as estimated by simulation of the experiment, this value is close to the T_2 limit of the technique using an echo time of 10 ms. In contrast to silica and polyacrylamide, agarose is known to have a very open structure with pore sizes on the order of hundreds of cubic nanometers.[38] The more open structure, and hence reduced obstruction effect,[5,39] is qualitatively the reason for faster diffusion in agarose compared to polyacrylamide. A two-sided t-test at a 98% confidence level shows the two results are statistically different. In all three cases the experimental diffusion coefficient of copper sulfate is attenuated from that measured in free aqueous solution[40] (14 mM, 25 °C), 6.5×10^{-6} cm^2 s^{-1}. Remarkably, there is a very close agreement between the measured diffusion coefficient of copper sulfate in 1% agarose and a literature value for the diffusion coefficient of copper ion in a structurally related agar gel matrix,[41] 5×10^{-6} cm^2 s^{-1}.

(29) Margel, S. *Appl. Biochem. Biotechnol.* **1983**, *8*, 523–539.
(30) Nilsson, K.; Scheirer, W.; Katinger, H. W.; Mosbach, K. *Methods Enzymol.* **1986**, *121*, 352–360.
(31) Freeman, A. *Methods Enzymol.* **1987**, *135*, 216–222.
(32) Ogden, R. C.; Adams, D. A. *Methods Enzymol.* **1987**, *152*, 61–87.
(33) Andrews, A. T. *Electrophoresis: Theory, Technique, and Biochemical and Clinical Applications*; Oxford Science: Oxford, England, 1986.
(34) *Modern Size Exclusion Chromatography*; Yau, W. W., Kirkland, J. J., Bly, D. D., Eds.; Wiley: Chichester, England, 1979.
(35) *Chromatography*; Heftman, E., Ed.; Elsevier: Oxford, England, 1983.
(36) Rothe, G. M.; Maurer, W. D. In *Gel Electrophoresis of Proteins*; Dunn, M. J., Ed.; John Wright: Bristol, England, 1986; p 47.
(37) Reference 1, p 150.
(38) Belton, P. S.; Hills, B. P.; Raimbaud, E. R. *Mol. Phys.* **1988**, *63*, 825–842.
(39) Muhr, A. H.; Blanshard, J. M. *Polymer* **1982**, *23*, 1013–1026.
(40) Eversole, W. G.; Kindswater, H. M.; Peterson, J. D. *J. Phys. Chem.* **1942**, *46*, 370–375.
(41) Lee, R.; Meeks, F. R. *J. Colloid Interface Sci.* **1971**, *35*, 584–592.

A trend similar to that observed for copper sulfate is present in the 4-amino-TEMPO diffusion results (Table II). The diffusion coefficient measured in a 1% agarose gel is larger than that measured in a 10% polyacrylamide gel. The diffusion coefficients (and 95% confidence intervals) are $(2.7 \pm 0.2) \times 10^{-6}$ cm^2 s^{-1} in 10% polyacrylamide and $(4.0 \pm 0.4) \times 10^{-6}$ cm^2 s^{-1} in 1% agarose. The two diffusion coefficients are statistically different when compared by a two-sided t-test at a 98% confidence level.

Not only do the measured diffusion coefficients in both media show the expected trend, agarose faster than polyacrylamide, but the larger size of the 4-amino-TEMPO, and thereby its increased frictional coefficient, results in a consistently smaller diffusion coefficient in both media. Thus the 4-amino-TEMPO diffusion coefficient is approximately 80% of that measured for copper in both media. Due to the fundamentally different nature of the two probes, charged versus uncharged and considerations of possible counterion effects, no more than a qualitative comparison is appropriate at this juncture. However, a quantitative examination of diffusion in either of these media would be possible using the inversion recovery imaging sequence; such experiments would require better temperature control and should focus on systematic changes in the gel matrix (via the percent composition) while employing the same paramagnetic probe. Alternatively one could systematically change the probe size while maintaining the gel matrix constant.

Conclusion

In conclusion we wish to emphasize the generality of the method. Although it relies on use of a paramagnetic substrate, a large number of transition metals and stable free radicals (or molecules labeled with these moieties)[42,43] are paramagnetic[9] and of potential interest. One of the salient properties of the method is its dependence on only one paramagnetic species in what may be a rather complicated molecular and environmental milieu.[1-3,44-47] The experiment is relatively fast (90 min) largely because it is possible to track a concentration, near the leading edge of the diffusion front, over a very small distance (3 mm). This compares favorably to many diffusion experiments which can take hours or days when large concentration differences over significant distances are required for detection.[48] The ease of the measurement and the small size of the sample means experiments of this type should be possible on many NMR spectrometers equipped with an imaging accessory.

Future work in this laboratory will encompass (1) extension of the technique to two spatial dimensions using a fast inversion recovery sequence, (2) diffusion measurements in model cellular tissue, and (3) examination of the effect of probe size on diffusion with large labeled probes.

Experimental Section

Aqueous Gels. Polyacrylamide gels were formed, over 24 h, from a 90:9.5:0.5. mixture (50 mL) of water, acrylamide, and bisacrylamide, using ammonium persulfate (Aldrich) as initiator (100 mg) and N,N,N′,N′-tetramethylenediamine (Aldrich) as accelerator (100 μL). The gel precursor solution was prepared by dilution of a stock 40% solution of acrylamide/bisacrylamide (Camlab). Water used in this preparation, and all others, was distilled, deionized, and degassed. Gels were cast as right cylinders in a 16 mm i.d. perspex cylinder 55 mm in height, sealed at the bottom. Water soluble byproducts of the reaction were removed by equilibration, over several days, in a large reservoir of water. Samples prepared for T_1 calibration were pre-equilibrated in large volumes of paramagnetic reagent (copper sulfate and 4-amino-TEMPO, Aldrich) solution at the appropriate concentrations for several days.

Agarose (Aldrich) gels, 1%, were prepared by addition of a calculated volume of water to the dry powder, and the resulting suspension was stirred for approximately 60 min. The mixture was heated under reflux for 30 min before casting in the desired mold (18.2 mm i.d. perspex cylinders, 55 mm in height), and the resultant samples were passively cooled to 21 °C. Samples for T_1 calibration experiments were prepared directly from stock solutions of copper sulfate and 4-amino-TEMPO.

Silica gels (Merck, silica 60) were prepared by addition of silica to gently stirred aqueous solutions in 17 mm o.d. glass vials, 60 mm in height. The resulting mixture was allowed to settle for 1 h and the excess water carefully removed by a syringe. Samples required for calibration experiments were prepared from stock solutions of copper sulfate. Changing the volume ratio of copper sulfate solution to dry silica did not significantly change the measured T_1.

Measurements. Polyacrylamide and agarose gel samples were cut to between 2 and 3 cm in length with a rigid thin wire or surgical scalpel and a guide to ensure that right cylinders with sharp edges were formed. Silica gel samples formed right cylinders, under gravity, as the particles settled after stirring. Careful handling ensured these interfaces were undisturbed prior to measurement. Polyacrylamide gels were inserted into a 16 mm i.d. perspex cylinder 55 mm in height, sealed at the bottom, vertically positioned inside a modified split ring NMR resonator.[49] Agarose samples were inserted into an 18 mm i.d. perspex cylinder 55 mm in height, sealed at the bottom inside the same or a similar NMR resonator. Silica gel samples remained in the original sample vials. The 180° pulse was calibrated before addition of approximately 5 mL (several cm) of paramagnetic solution to the perspex cylinder marked the beginning of the experiment. The paramagnetic ion solution was carefully added to a 1-cm layer of water overlaying the silica gel samples to avoid disturbing the surface. Samples were not thermostated although the ambient temperature was controlled at 21.5 ± 0.5 °C. The 180° pulse length was stable over several hours; because of the small sample size, the 180° pulse was also spatially uniform.

The imaging experiment was performed using an Oxford Research Systems Biospec 1 (83.7 or 84.7 MHz) instrument with an Oxford Instruments 31-cm horizontal bore magnet and a home-built gradient set. In a typical experiment, a magnetic field gradient (8000 Hz/cm) applied parallel to the long axis of the sample gave a 5.21-cm field-of-view with a resolution of 0.2 mm per pixel (spectral width 41 667 Hz); echo time, t_e, was 10 ms. Stronger field gradients and faster digitization rates were sometimes used to increase resolution to 0.1 mm per pixel. Gradients were linear and were calibrated by imaging one-dimensional phantoms of known length. Profiles (128 in total) were collected every 40 s commencing immediately after addition of the tracer solution. Four acquisitions were commonly interleaved in one experiment by repeating the inversion pulse every 10 s and cycling the delay t_d in order to observe four different concentrations C'.

Data Processing. Experimental time domain NMR data was transformed and displayed on a Sun SPARC station using in-house software. Experiments were simulated with Mathematica on a NeXT cube. Experimental null points were determined either by automatic detection of the minimum value within a profile or by manual searching of selected profiles. Diffusion coefficients were calculated from eq 3 via the slope of a plot of null-point position versus $t^{1/2}$. The null points from all 128 profiles were used in the regression analysis performed automatically; in the semi-automated processing protocol, null points from a limited number of profiles were subject to the same regression analysis. These profiles were chosen on the basis of the symmetry about the null of the signal from the nearest neighbor pixels. No significant differences were observed between the result from the semi-automated and fully automatic analyses using the same input experiments.

Acknowledgment. We thank Dr. Herchel Smith for a generous endowment (T.A.C., L.D.H.) and a research studentship (A.E.F.), NSERC of Canada for a postdoctoral fellowship (B.J.B.), and Dr. Edmund Fordham (Schlumberger-Cambridge) for valuable discussions.

(42) Cerdan, S.; Lotscher, H. R.; Kunnecke, B.; Seelig, J. *Magn. Reson. Med.* **1989**, *12*, 151-163.
(43) Muetterties, K. A.; Hoener, B. A.; Engelstad, B. L.; Tongol, J. M.; Wikstrom, M. G.; Wang, S. C.; Eason, R. G.; Moseley, M. E.; White, D. L. *Magn. Reson. Med.* **1991**, *22*, 88-100.
(44) Henisch, H. K. *Crystals in Gels and Liesegang Rings*; Cambridge University Press: Cambridge, England, 1988.
(45) Brinker, C. J.; Scherer, G. W. *Sol-Gel Science: The Physics and Chemistry of Sol-Gel Processing*; Academic: London, 1990.
(46) Harris, P. *Food Gels*; Elsevier: London, 1990.
(47) *Reversible Polymeric Gels and Related Systems*; Russo, P. J., Ed.; ACS Symposium Series 350; American Chemical Society: Washington, DC, 1987.
(48) Harned, H. *Chem. Rev.* **1947**, *40*, 461-522.
(49) Hall, L. D.; Marcus, T.; Neale, B.; Powell, J.; Sallos, J.; Talagala, S. L. *J. Magn. Reson.* **1985**, *62*, 525-528.